Chemical and Process Engineering 2012, 33 (1), 167-183
DOI: 10.2478/v10176-012-0015-0

EXPERIMENTAL AND NUMERICAL INVESTIGATION OF ELECTROSTATIC SPRAY LIQUID-LIQUID EXTRACTION WITH IONIC LIQUIDS

Marek Krawczyk, Kamil Kamiński, Jerzy Petera*

Technical University of Lodz, Faculty of Process and Environmental Engineering,
ul. Wólczańska 213, 90-924 Łódź, Poland

A new concept of an electrostatic spray column for liquid-liquid extraction was investigated. An important problem for separation processes is the presence of azeotropic or close-boiling mixtures in their production, for example heptane with ethanol, since the separation is impossible by ordinary distillation. The use of ionic liquids (IL) as a dispersed solvent specially engineered for any specific organic mixture in terms of selectivity is a key factor to successful separation. As IL present particularly attractive combination of favorable characteristics for the separation of heptane and ethanol, in this work we use 1-butyl-3-methylimidazolium methyl sulfate [BMIM][$MeSO_4$]. Because of high viscosity and relatively high cost of IL a new technique was introduced, consisting in the electrostatically spray generation to enhance the mass transport between the phases. In order to optimally design the geometry of the contactor a series of numerical simulation was performed. Especially multi-nozzle variants for better exploitation of contactor volume were investigated. Experiments showed excellent possibility of control of the dispersion characteristics by applied voltage and thus control of the rate of extraction. The preliminary simulations based on our mathematical model for a three nozzle variant exhibited visual agreement with the theory of electrostatics.

Keywords: electrostatic spray, ionic liquids, liquid-liquid extraction, numerical simulation

1. INTRODUCTION

Ionic liquids are organic salts that are liquid at or near room temperature (T_m < 100 °C). There are a myriad of cation/anion combinations that can yield a liquid organic salt. Figure 1 illustrates a few of the common classes of ionic liquids, *viz.* imidazolium, pyridinium, and quaternary phosphonium and ammonium. These combinations can be molecularly engineered for specific extraction or reaction tasks, through changes in physical properties, *e.g.* viscosity, solubility, H-bond acceptor/donor, acidity/basicity, co-ordination properties, etc. It has been estimated that nearly 10^{14} unique cation/anion combinations are possible (Holbrey and Seddon, 1999). Negligible vapor pressure also results in highly-elevated flash points, which extends safety to the decomposition temperature (>300 °C). Because of these properties, ionic liquids have been touted as potential "green" solvents.

An important problem for industrial processes is the presence of azeotropic or close-boiling mixtures in their production, for example heptane with ethanol, since the separation is impossible by ordinary distillation. Extractive distillation is the most widely used process to remove the components in the azeotropic system, but this process needs energy to obtain a fluid phase system. Nevertheless, the liquid–liquid separation leads to an environmentally friendly extraction process of the azeotropic mixture of heptane + ethanol as an alternative to azeotropic distillation, pervaporation and reverse

*Corresponding author, e-mail: jerzy.petera@.p.lodz.pl

osmosis, where these procedures require the use of large amounts of energy, volatile organic compounds, or high pressures.

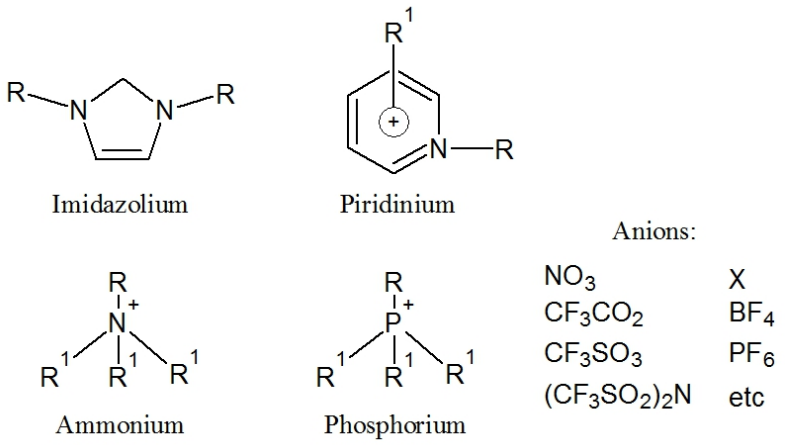

Fig. 1. Structure of common ionic liquids

Preliminary studies of activity coefficients at infinite dilution of the methylimidazolium-based ILs have in their favor the low activity coefficients of ethanol and the high ones of heptanes (Domanska and Marciniak, 2007; Foco et al. 2006). As these results suggest, these ILs are selected as solvents for mixtures of heptane with ethanol. Furthermore, alkylsulfateimidazolium derivates (Holbrey et al. 2002) are the most promising ILs to be applied in industrial processes since they can be easily synthesised in a halide-free way at a reasonable cost, are chemically and thermally stable, and have low melting points and relatively low viscosity. As IL present a particularly attractive combination of these characteristics for the separation of heptane and ethanol, in this work we study the behaviour of 1-butyl-3-methylimidazolium methyl sulfate [BMIM][$MeSO_4$].

Despite favorable thermodynamic and chemical properties of certain ionic liquids there are two fundamental challenges to the direct application of ionic liquids. One is the high viscosity exhibited by many of the ionic liquids solvent (Ahosseini et al. 2008; Ahosseini and Scurto, 2008). Second is the relatively high cost of ionic liquids compared with conventional solvents. As such, large inventories of these ILs in conventional extraction towers would not be suitable.

For liquid-liquid extraction, the method of transport between the two liquid phases will be diffusion, which is generally very slow. The mass transfer can be increased by convection and mechanical agitation, and one or both of these is necessary for reducing the time needed to reach equilibrium. In this experiment, ‘mixing’ is taken one step further by applying an electric field to the system. The ionic liquid is released from a nozzle(s) into an organic liquid mixture with a high voltage potential difference applied between the nozzle(s) and another electrode (usually at the bottom of the container). This creates an emulsion with very small droplet diameter which in turn increases the mass transfer rate, firstly by acceleration under electric field strength and secondly by developing the contact surface. These phenomena naturally increase the intensity of mass transport. A previous study showed qualitatively that the electrically enhanced technique applied in a liquid-liquid system reduces and narrows the size distribution. Production of very fine electrostatic dispersions of liquid drops of less than 1 micron in diameter has been demonstrated (Kaminski et al., 2010).

In order to better exploit the contactor volume from the efficiency of mass exchange more than one nozzle must be used. This creates an issue of equal distribution of the ionic liquid between the nozzles. Such a distributor has been built recently and a preliminary simulation has been performed on a prototype contactor in order to test the geometry from that point of view.

In this paper the numerical simulation is performed firstly for testing the equal distribution of the ionic liquid between the nozzles, and secondly another simulation was done for confronting the electrostatic theory with our own experiments of electrostatic spray production.

In parallel we conducted experiments in which we investigated various aspects of mass transfer phenomena between the ionic liquid (dispersed electrically) and the organic continuous phase. Especially the extraction efficiency as a function of applied electrical potential magnitude is of the main interest in respect to the process control.

2. EXPERIMENTAL

To test extraction efficiency using the electrostatic spray column an experiment with single nozzle (without distributor) was done. The experimental setup is presented in Figure 2. It consists of a cylindrical glass column with a volume of a little over 2 liters. There is a threaded hole at the bottom of the cylinder where a valve was attached for easy separation of the heavier extract phase. 2 cm above the bottom, on the side of the column, there is a port for the electrode and it is sealed with a silicon plug. The red wire leaving the electrode is connected to the 100 W generator (the gray rectangular box) which is able to produce electric potential up to 30 kV. The top of the column is also sealed with a rubber plug that holds the nozzle (made from a needle) through which the ionic liquid is pumped. For ionic liquid dosing an infusion pump is used (the blue syringe pump behind the column). The needle is grounded and connected to the generator along with the electrode near the bottom of the column. The system of the nozzle and the electrode is immersed in a liquid organic mixture, which together constitute a mass exchange contactor. The generated electric field is placed between the grounded nozzle and the high-voltage electrode. The distance between them can be adjusted and is determined by the volume of the used organic mixture. In the experiment presented in Figure 2 half of the contactor capacity is in use and the spacing between the tip of the nozzle and the electrode is about 10 cm. Additionally, for better presentation of flows coming in and out of the contactor, a scheme of experimental setup is showed in Figure 3.

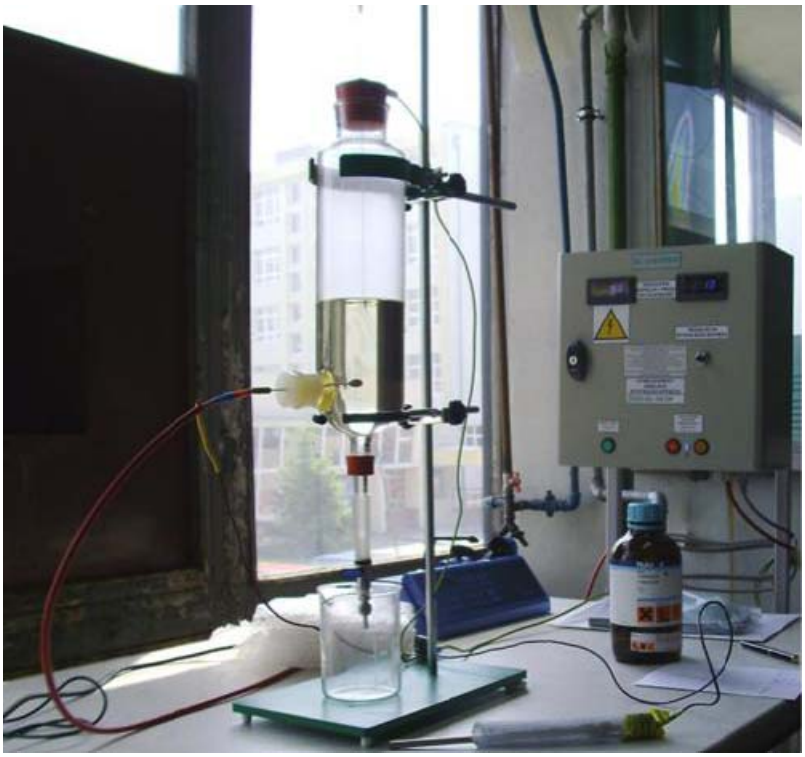

Fig. 2. Experimental setup

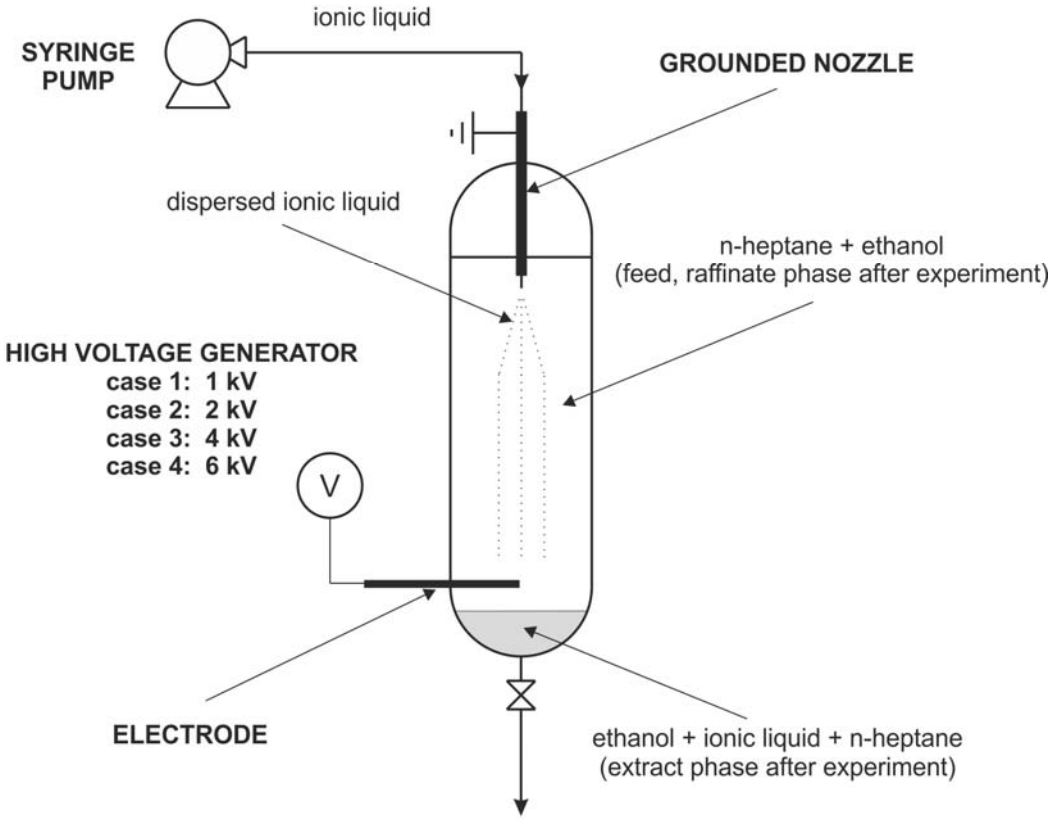

Fig. 3. Scheme of general idea of the experiment

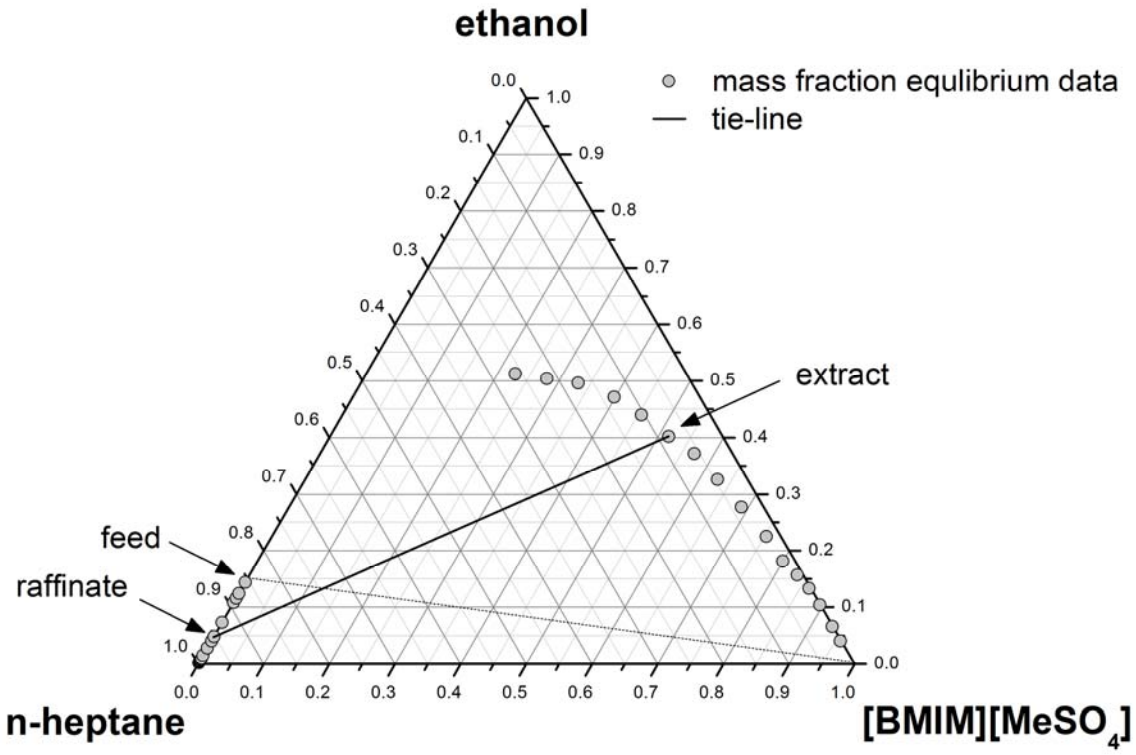

Fig. 4. Equilibrium data [mass fraction] for ternary system of ethanolheptane[BMIM][MeSO4]

In the performed series of experiments an organic mixture of ethanol and n-heptane was used as the continuous phase and ionic liquid [BMIM][MeSO4] (1-butyl-3-methylimidazolium methyl sulfate) as

the dispersed phase. The amounts of the used chemicals were estimated using the lever rule on the basis of literature data presented in Figure 4 (Pereiro and Rodriguez, 2008). At the beginning the contactor was filled with 1 dm^3 of organic mixture (15% by mass of alcohol). In each experiment the infusion pump dozed 85 ml of the ionic liquid with a constant flow rate of 20 ml/h. For the tie-line indicated in Figure 4 the concentration of ethanol in the organic mixture obtained after extraction was about 4,8%.

The efficiency of ethanol extraction from the organic mixture was tested in four cases with a different voltage applied in the contactor: 1 kV, 2 kV, 4 kV and 6 kV. To measure the concentration of ethanol in the mixture with n-heptane after each experiment, a gas chromatography was used. The following setup of the gas chromatograph was applied: Quadrex 007-1 15m×0,1mm×0,1μm column, FID detection, oven temperature 60 °C, sample dozing temperature 250 °C, N_2 as the mobile phase.

The gas chromatography measurements of ethanol concentration in the organic mixture after each of the experiments are presented in Table 1.

Table 1. Measurements of ethanol concentration in the organic mixture (raffinate phase)

	Applied voltage [kV]	Ethanol concentration [% m/m]
Case 1	1	8.1
Case 2	2	4.5
Case 3	4	3.5
Case 4	6	3.4

It can be noticed that the higher voltage is applied, the lower concentration of alcohol is obtained. It shows that increasing electric field strength in the contactor allows to conduct a better separation (purification) of the organic mixture. However, comparing the results for 4 kV and 6 kV, it is visible that for the specified distance between the grounded nozzle and the high voltage electrode there is a maximum voltage level above which further improvement is not achievable. The measured concentration values can be explained with the size of dispersed phase droplets obtained in each case. Figure 5 presents an electro-spray produced for each voltage value, except for 6 kV as the thick fog produced in this case would blare the image.

The results prove that changes in electric potential in the column allow to control the dispersion level of the ionic liquid. When 1 kV is applied to the high voltage electrode only discrete droplets are obtained in the contactor. With the increase of the electric field strength finer droplets are produced (2 kV) and finally with the use of 4 kV or 6kV (not presented in Figure 5) an emulsion appears in the column. The overall efficiency of mass transfer in the batch contactor depends on the interfacial area produced in the experiment. The higher voltage is applied the finer droplets are obtained which results in enhancing the interfacial area between the continuous and dispersed phases and improves extraction efficiency. The comparison of the results for the electrostatic spray column with 2 kV, 4 kV and 6 kV (presented in Table 1) with data from Figure 4 proves that the column is very efficient in reaching at least the same concentration of ethanol as the equilibrium state. The obtained lower concentrations in contactor after the experiments are probably caused by differences in temperatures. The equilibrium triangle is prepared for 25 °C and the experiments were performed in laboratory ambient temperature which was several degrees higher.

Size and diameter distribution of the dispersed phase are crucial for the efficiency of all operations including mass transfer (i.e. extraction). Electrically driven separation in which dispersion quality can be controlled with the level of applied voltage seems to be an attractive technique competitive to the well-known classic methods (i.e. distillation, extraction with mechanical agitation).

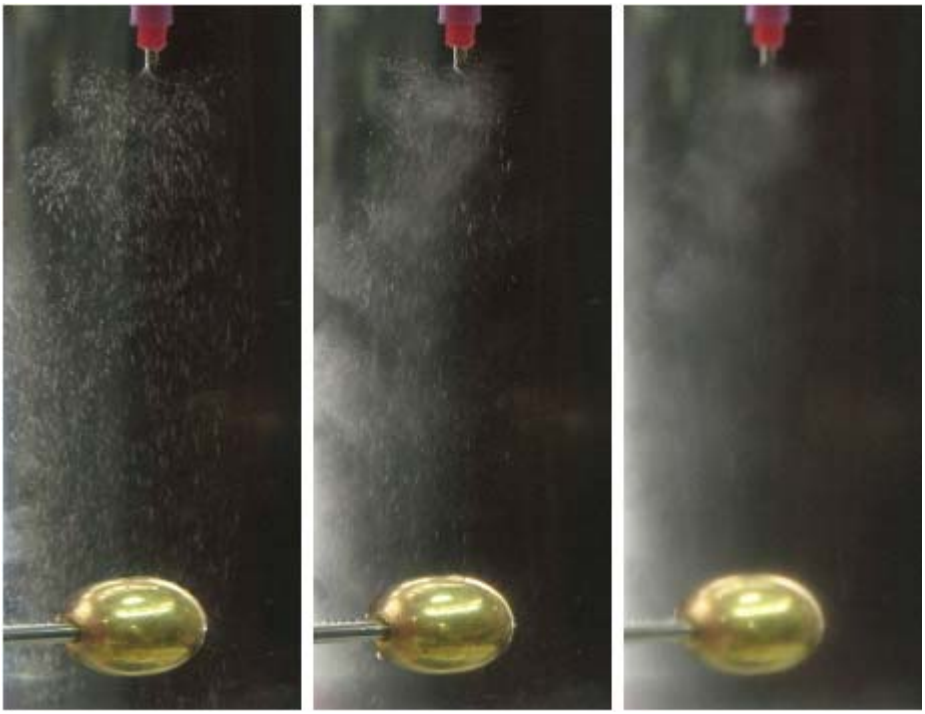

Fig. 5. Electro-spray produced for application of different electric potential in the contactor: from the left 1 kV, 2 kV, 4 kV

3. NUMERICAL SIMULATION FOR IMPROVEMENT OF THE EXTRACTION PROCESS

For the efficiency improvement of the presented electrostatic spray column the number of nozzles used in the contactor should be increased. A single nozzle did not make use of the full contactor volume. The zone of the mass exchange was obviously limited to the spray region situated naturally in the middle over the shortest way between the two electrodes. Thus a form channeling could be observed. A multi-nozzle design could allow to obtain higher flow rates at the same contactor volume.

We have built recently a new multi-nozzle contactor for efficient exploitation of the full volume. An issue of equal distribution of the ionic liquid appeared since not all the electrodes were supposed to be in the same flowing condition. In order to correctly formulate the design assumptions some numerical simulations were done for laminar regime. However, we want to emphasise that our aim was not to simulate details of the flow but only the mass conservation in the flow through the distribution container.

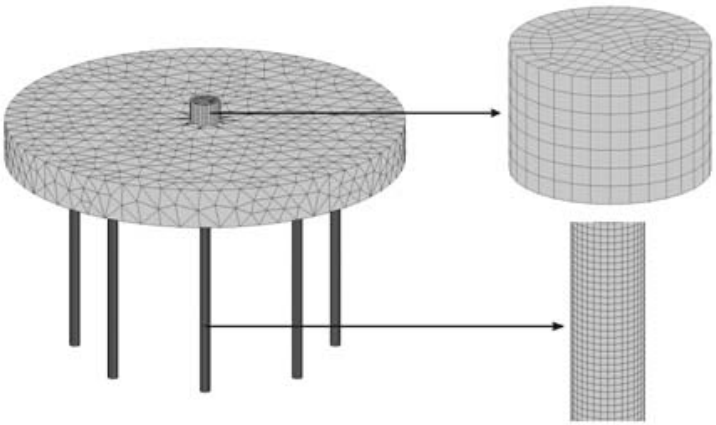

Fig. 6. Computational domain and the mesh together with a zooming of inlet and outlet details

3.1. Computation domain and mesh

The computation domain consisted of the inlet pipe, distribution container and the outlet capillaries, as shown in Figure 6. The figure shows also the computational mesh created by commercial software Ansys Meshing 13, containing 244944 elements and 268093 nodes. A zooming of the inlet pipe and outlet capillary is also shown. Incidentally, the area of the inlet is equal to the sum of all outlet areas.

The main dimensions of the computational domain are presented in Figure 7.

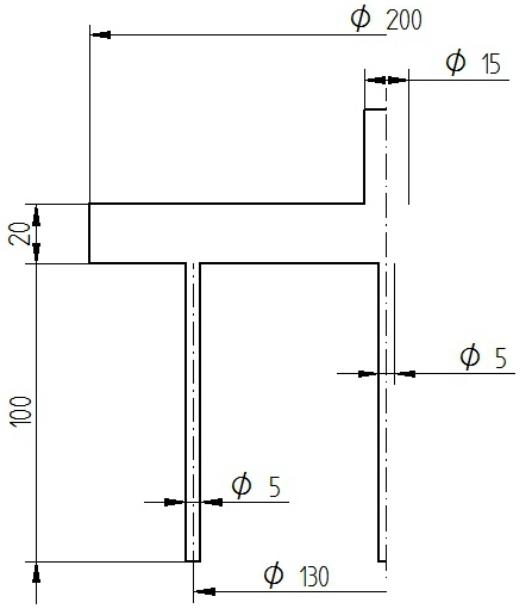

Fig. 7. Main dimensions of the computation domain (in mm)

3.2. Boundary conditions

The following simple boundary conditions were imposed on the computational domain with the terminology consistent with the ANSYS Fluent 13:

- *mass flow inlet* meaning the mass flow rate at the inlet is given, relating to the normal velocity component as

$$\rho_f \cdot v_n = \frac{\dot{m}_{in}}{A_{in}} \tag{1}$$

- *pressure outlet* (*gauge pressure*) meaning zero static pressure at the outlet of all capillaries,
- *stationary wall* at the other boundaries of the domain, meaning “no slip” condition at the real walls.

The boundary conditions are illustrated in Figure 8.

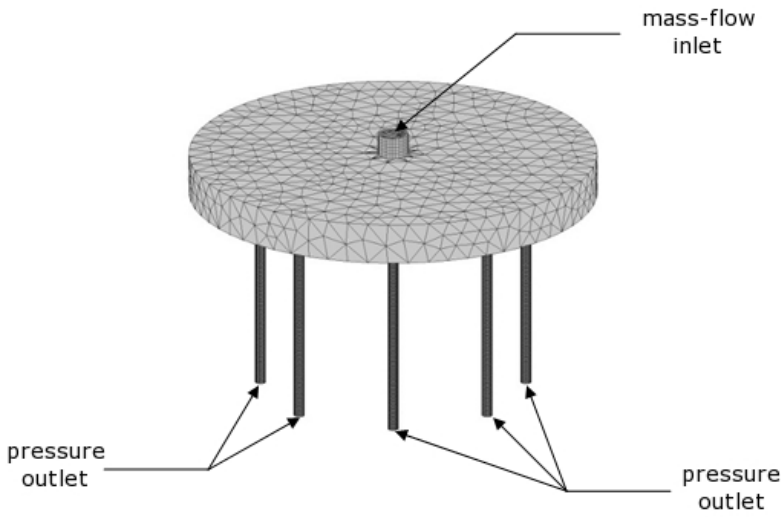

Fig. 8. Boundary conditions imposed on the computational domain

3.3. Material properties of the ionic liquid

As mentioned before, the dispersed medium was an ionic liquid otherwise used for an extraction process of ethanol from some organic mixtures, 1-Buthyl-3-methylimidazolium methanesulfonate [BMIM][$MeSO_4$] with the formula showed in Figure 9.

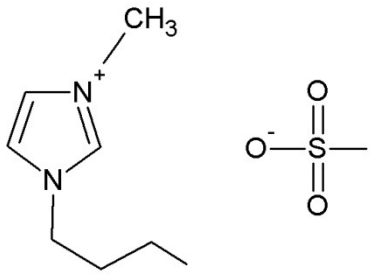

Fig. 9. Chemical formula for [bmim][$MeSO_4$] (ChemicalBook, 2011)

Table 2 presents some basic physical properties of the ionic liquid (Fernandez et al., 2008).

Table 2. Physical properties of [BMIM][$MeSO_4$] used in the computations

Physical property	Unit	Value
Molar mass	g/mol	250.32
Viscosity at room temperature	Pa·s	0.2138
Density at room temperature	kg/m^3	1212.9

3.4. Computational variants

Table 3 below shows the computational variants for determining the equal distribution of flow currents through all the capillaries, particularly between the central and peripheral ones.

Table 3. List of computational variants

No.	Volumetric flowrate [ml/h]	Mass flowrate [kg/s]
1	20	$6.738 \cdot 10^{-6}$
2	25	$8.423 \cdot 10^{-6}$
3	30	$1.011 \cdot 10^{-5}$
4	35	$1.179 \cdot 10^{-5}$
5	40	$1.348 \cdot 10^{-5}$
6	50	$1.685 \cdot 10^{-5}$
7	60	$2.022 \cdot 10^{-5}$
8	70	$2.358 \cdot 10^{-5}$
9	80	$2.695 \cdot 10^{-5}$
10	90	$3.032 \cdot 10^{-5}$
11	100	$3.369 \cdot 10^{-5}$

3.5. ANSYS Fluent settings

The numerical calculations were performed using the well-known commercial standard ANSYS Fluent 13. In this case the Pressure-Based solver was used for the steady state conditions. We want to emphasise that we wanted to test only equal mass distribution between the nozzles in view of future contactor design.

Table 4. Mass flow rates at all the nine outlets from the domain

Outlet No	Variant 1. Mass flow rate [kg/s]	Variant 9. Mass flow rate [kg/s]
1	$7.4644 \cdot 10^{-7}$	$3.7324 \cdot 10^{-6}$
2	$7.4787 \cdot 10^{-7}$	$3.7395 \cdot 10^{-6}$
3	$7.4575 \cdot 10^{-7}$	$3.7290 \cdot 10^{-6}$
4	$7.4726 \cdot 10^{-7}$	$3.7363 \cdot 10^{-6}$
5	$7.5196 \cdot 10^{-7}$	$3.7595 \cdot 10^{-6}$
6	$7.5118 \cdot 10^{-7}$	$3.7556 \cdot 10^{-6}$
7	$7.4976 \cdot 10^{-7}$	$3.7488 \cdot 10^{-6}$
8	$7.4927 \cdot 10^{-7}$	$3.7324 \cdot 10^{-6}$
central	$7.4853 \cdot 10^{-7}$	$3.7395 \cdot 10^{-6}$

For the *Pressure-Velocity Coupling* the SIMPLE algorithm was used with the default settings including the *Under-Relaxation Factors. Convergence Absolute Criteria* was set to 0.0001, giving the convergence after ca 1000 iterations.

Table 5 presents a comparison between mass flow rates at the inlet on the one hand and the sum of outlets on the other, for all the variants mentioned above. This proves that the overall mass conservation is fulfilled.

Table 5. Comparison between mass flow rates at the inlet and the sum of outlets, for all the computational variants

Variant Number	Inlet [kg/s]	∑outlets [kg/s]
1	$6.738 \cdot 10^{-6}$	$6.7380006 \cdot 10^{-6}$
2	$8.423 \cdot 10^{-6}$	$8.4230005 \cdot 10^{-6}$
3	$1.011 \cdot 10^{-5}$	$1.01100005 \cdot 10^{-6}$
4	$1.179 \cdot 10^{-5}$	$1.17900004 \cdot 10^{-5}$
5	$1.348 \cdot 10^{-5}$	$1.34800008 \cdot 10^{-5}$
6	$1.685 \cdot 10^{-5}$	$1.01100005 \cdot 10^{-5}$
7	$2.022 \cdot 10^{-5}$	$2.02200006 \cdot 10^{-5}$
8	$2.358 \cdot 10^{-5}$	$2.35800006 \cdot 10^{-5}$
9	$2.695 \cdot 10^{-5}$	$2.69500007 \cdot 10^{-5}$
10	$3.032 \cdot 10^{-5}$	$3.03200005 \cdot 10^{-5}$
11	$3.369 \cdot 10^{-5}$	$3.36900021 \cdot 10^{-5}$

A more important issue (at least from the point of view of the real apparatus being actually built) is the equal distribution of the mass flow rate at each capillary outlet. Particularly the central capillary which works in different conditions than the peripheral ones is supposed to transport the same mass. Table 5 proves that the central capillary in fact fulfils the requirement of equal mass distribution as the points in the figure for each of 11 variants in fact coincide.

4. NUMERICAL SIMULATION AIMED AT A PRELIMINARY TESTING OF THE EXTRACTION PROCESS

Before building the contactor mentioned above a new (provisional and thus cheaper) distributor was built to test the viability of the process especially from the inter-electrode distances point of view. Instead of nine capillaries as presented in Figure 6 it consisted of only three nozzles, all at the same electric potential. They created an electro-spray as a result of imposing electric field between the nozzles and another high voltage electrode fixed below at contactor bottom. Further CFD simulations were performed for the computational domain containing three inlets of ionic liquid corresponding to three nozzles.

4.1. Computation domain and mesh

The computation domain was chosen naturally according to Figure 10. Figure 11 shows also the computational mesh created by commercial software ANSYS Meshing 13, containing 57245 elements and 85770 nodes. A zooming of the area near the (small) nozzles is also shown. The 3D model was

created using a commercial software ANSYS DesignModeler 13 (component of the ANSYS Workbench 13).

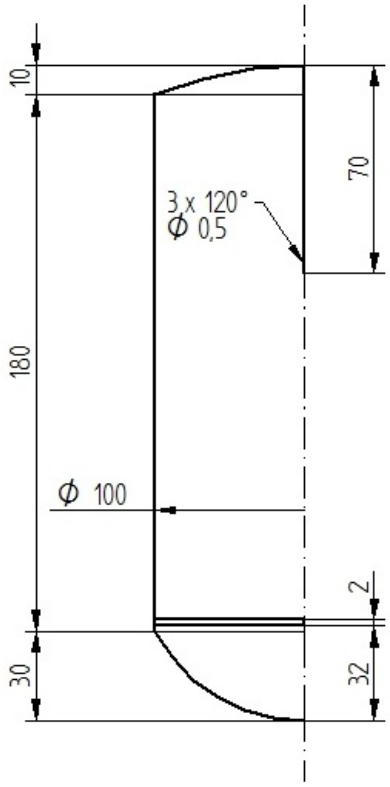

Fig. 10. Axial section of the contactor together with the main dimensions (in mm)

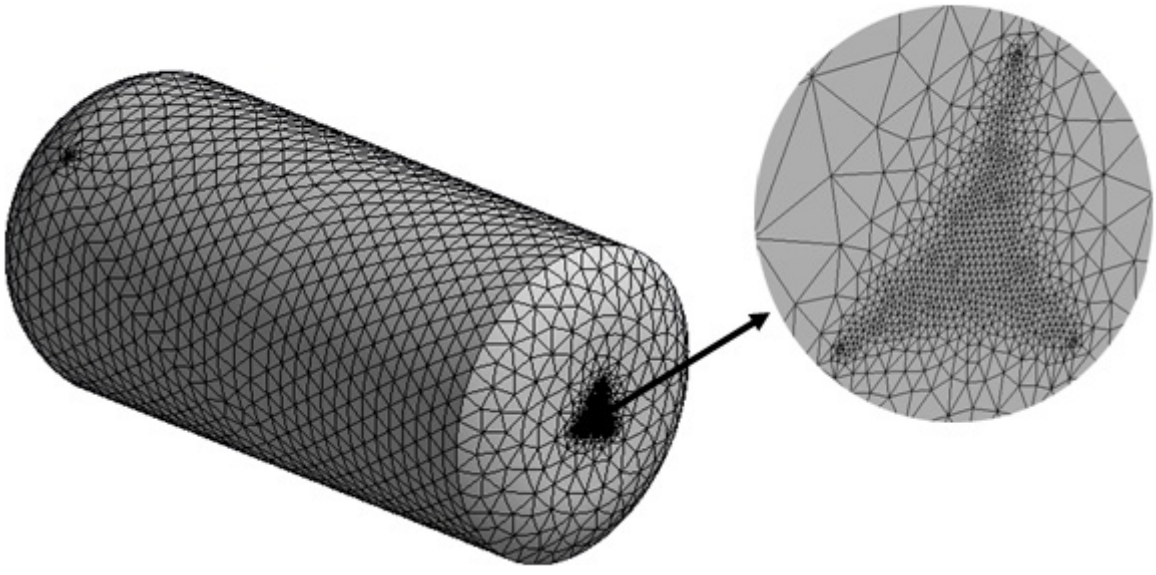

Fig. 11. Computational domain and the mesh together with a zooming of outlet details

4.2. The boundary conditions

For simplicity purposes, in order to simulate the electric potential field, the analogy between the steady thermal conduction and the electric potential conservation was used. In fact the two corresponding

equations are formally identical. For the electric potential conservation we have the well known Poisson differential equation:

$$\underline{\nabla} \cdot \left(\varepsilon_r \underline{\nabla} \Phi \right) = -\frac{\sigma}{\varepsilon_0} \tag{2}$$

where Φ is the electric potential, ε_r, the relative permittivity of materials (dielectric liquid), $\varepsilon_0 = 8.842 \cdot 10^{-12}$ the dielectric constant of the free space, σ – the electric space free charge density, here $\sigma = 0$.

If we formally substitute temperature for Φ, and the thermal conductivity for ε_r then the steady conduction equation is obtained. Thus the boundary conditions used in our solutions to the above equation (formally in ANSYS for temperature and heat flux), were (3a) of the Dirichlet type: Φ prescribed on the part Γ_ϕ of the total boundary Γ, belonging to the electrodes, $\Phi = 0$ on the earthed three electrodes,

$$\Phi = \Phi_{HV} \tag{3a}$$

$$\mathbf{E} \cdot \mathbf{n} = h \tag{3b}$$

where **E** is the electric field strength vector,

$$\mathbf{E} = -\underline{\nabla} \Phi \tag{4}$$

and **n** is the outward unit vector normal to the boundary. h is a function of position on the part Γ_h of the boundary. We assumed that h is simply zero, which means no leakage of the electric field at the wall.

Generally, the following forces determine the motion of a charged droplet released in a dielectric liquid with the possible presence of other charged droplets. The first group can be classified as electrical forces resulting from the particular mechanisms listed as follows: electrophoresis (EP), dielectrophoresis (DEP), electroosmosis (EOS). A detailed description and formulae were given in our previous paper (Petera et al., 2007).

Here we are repeating only the formula for electrophoresis, as the most important one, which involves force acting on a charged particle/droplet due to an external electric field with the force proportional to the electric field strength.

$$\mathbf{F}_{EP} = q\,\mathbf{E} \tag{5}$$

where q is the electric charge of the particle/droplet. It may change according to the very well-known rule (for constant permittivity ε_r and conductivity κ of the liquid) (Bailey, 1988):

$$q = q_0 \exp\left(-t/\lambda\right) \tag{6}$$

where $\lambda = \varepsilon_0 \varepsilon_r / \kappa$ is the relaxation time of the dielectric liquid. **E** is the resultant electric field strength from the externally applied electric potential and from contribution from other droplets in the close neighborhood.

We assume on the basis of our previous investigations (Petera et al., 2009) that the charged droplets follow mainly the following force balance

$$m_d \frac{\mathrm{d}\mathbf{u}_d}{\mathrm{d}t} = \mathbf{F}_{EP} + \mathbf{F}_D + \mathbf{F}_B \tag{7}$$

where $\mathbf{F}_D$ is the drag force and $\mathbf{F}_B$ is the buoyancy force.

The boundary conditions are illustrated in Figure 12.

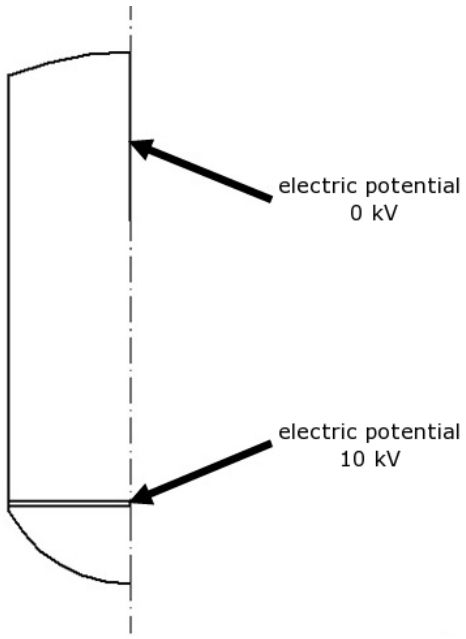

Fig. 12. Boundary conditions for the electric field potential imposed by ANSYS Mechanical software

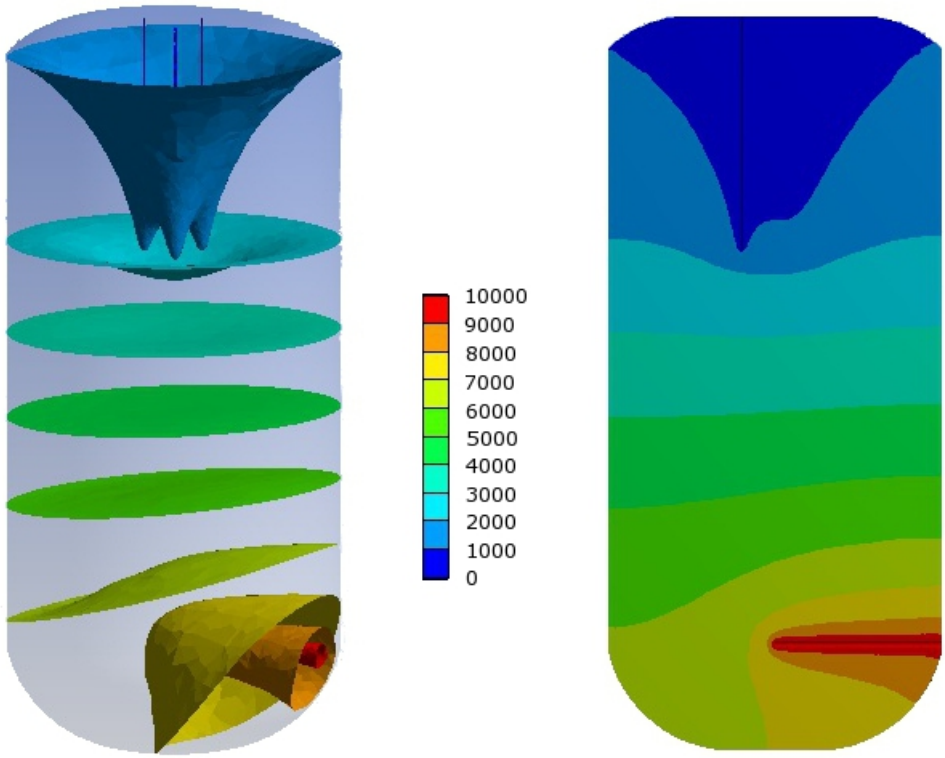

Fig. 13. The electric potential field (range from 0 to 2 kV) in the experimental contactor presented in Figure 11. Equipotential surfaces in 3D geometry (left) and contours in the contactor centerline 2D section (right)

4.3. Simulation results

In order to show an agreement between the theoretical electrostatic fields, namely the electric potential and electric field strength, the numerical solution of the boundary value problem, represented by Equations (2-7), are shown in Figure 13 and Figure 14. We want to confirm experimentally that the

simplified electrostatic model follows generally the experiments done so far. This will provide guide for designing a bigger multi-nozzle contactor.

Thus the next Figure 15 represents a visual comparison between the distribution of electric field strength at the three nozzles on the left-hand side with the electro-spray generated by the same electric field obtained in the real experiment. Because the droplet motion should follow the dynamic equation (7) we should observe in principle three different zones occupied by sprays, each associated with the corresponding nozzle. The shape of each spray must correspond with the tendency of electrostatic field distribution.

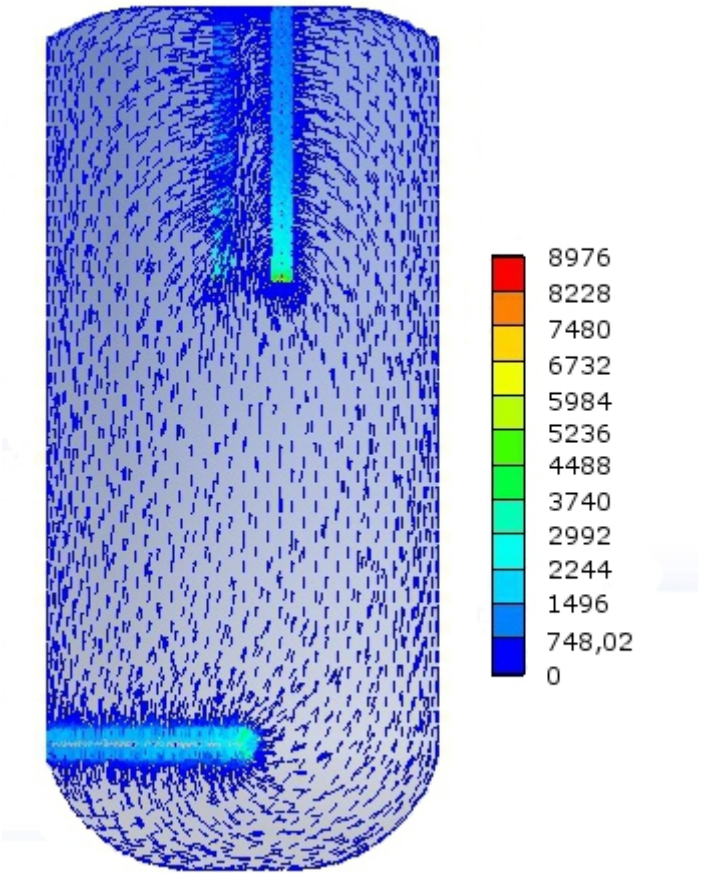

Fig. 14. The simulated electric field strength (V/m) in the contactor space in form of arrows

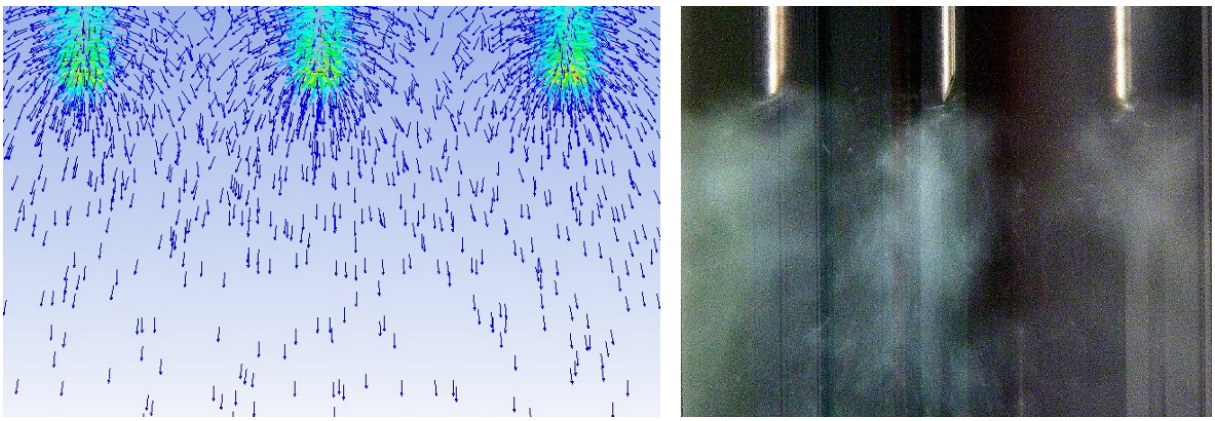

Fig. 15. Visual comparison between the distribution of electric field strength at the three nozzles on the left-hand side with the electro-spray generated by the same electric field obtained in the real experiment. (The legend for the left-hand side is identical with that in Figure 14)

We want to emphasise that according to our model the electric field strength on the left hand side should determine the shapes of the clouds on the right. For an explicit confirmation an additional simulation of the dispersed phase volumetric fraction in the spray was done for matching visually the experimental counterparts. We wanted to confirm our understanding of the electrically driven spray in the contactor. We used our own software and mathematical model formulated in the Lagrangian framework described elsewhere (Petera et al., 2007; 2009), based on the discrete trajectory tracking and statistically defining the droplet "clouds" around each center (mean) trajectories. Figure 16 shows the results of the simulation in form of the dispersed phase volumetric fraction contours together with the mean trajectories of the clouds. A quite accurate match between the simulation and the experimental pictures in Figure 15 demonstrates the validity of the approach and this should provide a valuable tool for liquid-liquid contactor design. The most intensive electric field strength occurs, as expected near the nozzles were the geometry curvature is biggest. However, the flow is released only from the orifice of each nozzle and the spray develops only below the nozzles, thus only a part of the electric field's strength is really utilised for droplet acceleration.

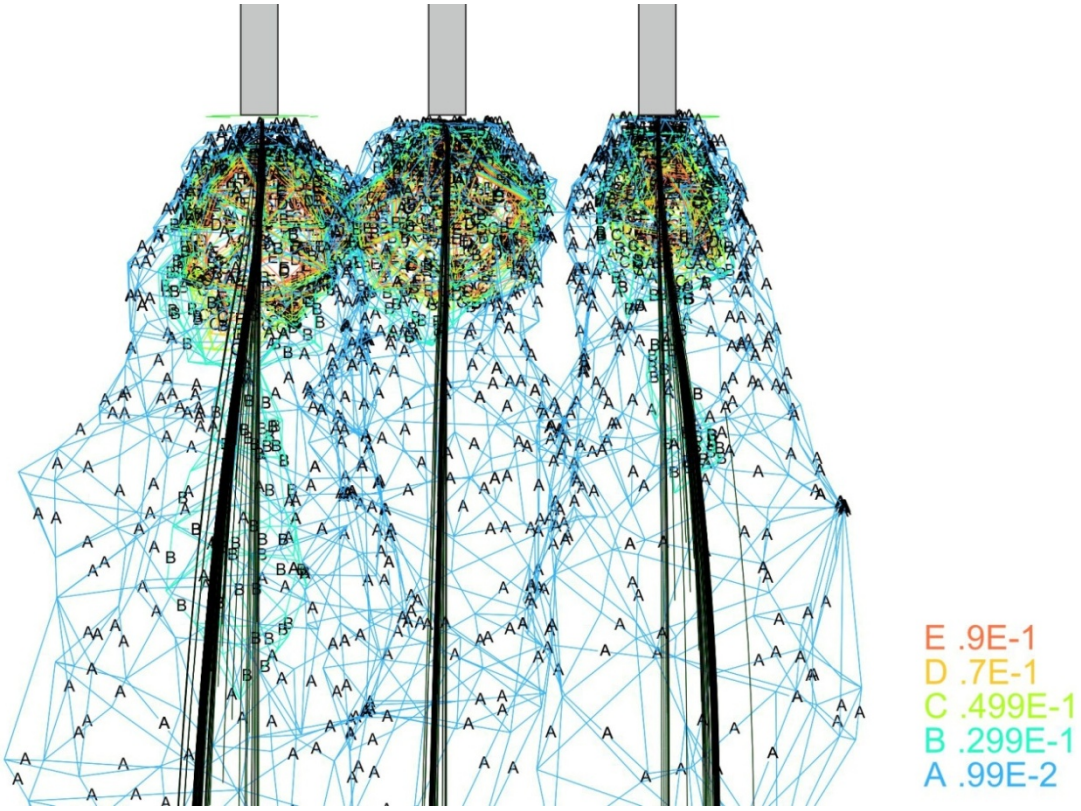

Fig. 16. The volumetric fraction of the dispersed phase contours together with the mean trajectories of the clouds (continuous black lines)

An interesting feature of the sprays can also be observed. As the droplets acquired the same charge there is a tendency of repulsion between separate sprays, which is also reflected in a distribution of the electric field's strength as well as in the simulated spray clouds.

7. CONCLUSIONS

This paper represents a report on the present stage of investigations on a new electrostatic spray liquid-liquid extraction column. Since the electro-spray operates in nearly electrostatic regime the power consumption is marginal (ultimate electric current was 3 mA for 6kV resulting in 100 Watts of generator power consumption). Thus the column should offer a low energy separation unit especially in

case of separating azeotropic organic mixtures as opposed to the traditional technology involving substantial energy consumption. Ionic liquids are chosen as green solvents of low hazard risk, offering high selectivity. They can also be individually tailored for specific mixtures.

The preliminary simulations of electrostatic multi-nozzle spray contactor proved the validity of the design assumptions. The mass flow rates divide equally between the nozzles despite apparently different situation of the central nozzle.

Electrostatic spray production experiments exhibit strong dependence of the average droplet diameter in the spray on the applied electric field (voltage). The results prove that changes in electric potential in the column allow to control the dispersion level of the ionic liquid. The overall efficiency of the mass transfer in the batch contactor depends on the interfacial area produced in the experiment. The higher voltage is applied the finer droplets are obtained which results in highly developing the interfacial area with very likely enhancing of interface phenomena during acceleration under electric force. This in turn improves extraction efficiency.

The usage of three (instead of one) nozzles offers much better exploitation of the contactor space (volume). In case of a single nozzle the channeling effect was visible and most of the volume was not exploited. The experiments showed that separate clouds of droplets formed from each nozzle slightly interfering with each other (repulsion) but visually followed the electric field's strength vectors. The simulations of the vector field and the clouds of droplets confirmed this hypothesis.

It is concluded that the simulation framework and its experimental verification will enable the development of optimal designs for intensified liquid-liquid electrostatic contactors without the need for expensive experimentation.

This research was supported by the Polish State Committee for Scientific Research by means of Grant No. N N209 228838.

SYMBOLS

A_{in}	area of inlet section, m^2
M_{in}	mass flow rate at the inlet, kg/s
m_d	particle/droplet mass, kg
q	electric charge of the particle/droplet, C
v_i	velocity at the inlet, m/s
v_n	normal velocity component at the inlet, m/s
v_o	velocity at the outlet, m/s
t	time, s
u_d	particle/droplet velocity, m/s

Greek symbols

σ	the electric space free charge density, C/m^3
ε_r	the relative permittivity of materials (dielectric liquid), -
κ	conductivity of the liquid, S/m
λ	the relaxation time of the dielectric liquid, s
Φ	electric potential, V

REFERENCES

Ahosseini A., Petera J., Weatherley L.R., Scurto A.M., 2008. Interfacial mass transport properties in biphasic ionic liquid systems. *ACS National Meeting,* Philadelphia, USA, 17-21 August 2008.

Ahosseini A., Scurto A. M., 2008. Viscosity of imidazolium-based ionic liquids at elevated pressures: Cation and anion effects. *Int. J. Thermophysics*, 29, 1222-1243. DOI: 10.1007/s10765-008-0497-7.

Bailey AG. 1988. *Electrostatic Spraying of Liquids*. Wiley, New York.

Domańska U., Marciniak A., 2008. Activity coefficients at infinite dilution measurements for organic solutes and water in the ionic liquid 1-butyl-3-methylimidazolium trifluoromethanesulfonate. J. Phys. Chem. B, 112, 11100–11105. DOI: 10.1021/jp804107y.

Fernandez A., Garcia J., Torrecilla J.S., Oliet M., Rodriguez F., 2008. Volumetric, transport and surface properties of [bmim][$MeSO_4$] and [emim][$EtSO_4$] ionic liquids as a function of temperature. *J. Chem. Eng. Data*, 53, 1518-1522. DOI: 10.1021/je8000766.

Foco G.M., Bottini S.B., Quezada N., de la Fuente J.C., Peters C.J., 2006. Activity coefficients at infinite dilution in 1-alkyl-3-methylimidazolium tetrafluoroborate ionic liquids, *J. Chem. Eng. Data*, 51, 1088–1091, DOI: 10.1021/je050544m.

Holbrey J.D., Reichert W.M., Swatloski R.P., Broker G.A., Pitner W.R., Seddon K.R., Rogers R.D., 2002. Efficient, halide free synthesis of new, low cost ionic liquids: 1,3-dialkylimidazolium salts containing methyl- and ethyl-sulfate anions. *Green Chem*, 4, 407–413. DOI: 10.1039/b204469b.

Holbrey J.D., Seddon K. R., 1999. Ionic liquids, *Clean Prod. Proc.*, 4, 223-236. DOI: 10.1007/s100980050036.

Kamiński K., Bachtel A., Petera J., 2010. High voltage electro-spray extraction from organic mixture using room temperature ionic liquids, *Inż. Aparat. Chem.*, 2, 61-62 (in Polish).

Pereiro A.B. , Rodriguez A., 2008. Azeotrope-breaking using [BMIM] [MeSO4] ionic liquid in an extraction column. *Sep.Purif. Technol.*, 62, 733-738. DOI: 10.1016/j.seppur.2008.03.015.

Petera J., Weatherley L.R., Hume A.P., Gawrysiak T., 2007. A finite element algorithm for particle/droplet trajectory tracking, tested in a liquid–liquid system in the presence of an external electric field. *Comp. Chem. Eng.*, 31, 1369–1388. DOI: 10.1016/j.compchemeng.2006.11.010.

Petera J., Weatherley L. R., Rooney D., Kaminski K., 2009. A finite element model of enzymatically catalyzed hydrolysis in an electrostatic spray reactor, *Comp. Chem. Eng.*, 144-161, DOI: 10.1016/j.compchemeng.2008.07.006.

ChemicalBook. Retrieved 08.09.2011 from http://www.chemicalbook.com.

Received 30 September 2011
Received in revised form 8 March 2012
Accepted 8 March 2012